Comparative study and calibration of sensors for the measurement of the liquid water content of clouds with small droplets

P. Personne, Brenguier J.L., Jean-Pierre Pinty, Y. Pointin

Comparative Study and Calibration of Sensors for the Measurement of the Liquid Water Content of Clouds with Small Droplets

P. PERSONNE, J. L. BRENGUIER, J. P. PINTY AND Y. POINTIN

L.A.M.P., University of Clermont II, 63170 Aubière, France

(Manuscript received 9 March 1981, in final form 12 August 1981)

ABSTRACT

Measurements of cloud liquid water content made with various probes reveal a disagreement between their results.

We show in this paper that comparisons between actual airborne measurements make it possible to define correction procedures which improve the accuracy of each probe.

1. Introduction

During the past few years, several kinds of probes have been used to determine the microphysical characteristics of natural and artificial clouds in airborne or wind tunnel measurements. These probes have been tested in the laboratory in order to determine their range of suitability and their respective limitations. However, it is not easy to reproduce in the laboratory the natural conditions of airborne measurements, especially the relative speed of the particles (100 m s^{-1}) nor is it easy to know the spectral characteristics of the droplet distribution with sufficient accuracy. We have therefore studied these probes *a posteriori* by comparing the results of measurements made over a wide range of clouds studied during the Precipitation Enhancement Project (PEP) and the West African Monsoon Experiment (WAMEX). An example of such comparisons concerning the liquid water content of small droplet clouds is given here. This example is mainly based on measurements made during the PEP 79 experiment.

2. Microphysical probes

a. Measurement of droplet spectra

The Forward Scattering Spectrometer Probe (FSSP) probe of the Particle Measuring System is based on the measurement of the laser light intensity scattered by each droplet. Droplets having diameters between 3 and 45 μm are sized and sorted into 15 classes of 3 μm width every 0.1 s by the electronic circuitry. The liquid water content is computed over the spectrum using relation

$$q_1 = \tfrac{1}{6}\pi \sum_{i=1}^{15} \rho n_{mi} D_i^3/(VAT), \qquad (1)$$

where n_{mi} is the number of droplets in the ith class of mean diameter D_i, V the relative velocity of particles, A the "true sampling area", T the sampling time, and ρ the density of water ($\rho = 1$); $n_{mi}/(VAT)$ represents the concentration N_{mi}.

The different characteristics of this probe have been tested in the laboratory. The rejection circuitry excludes particles crossing the beam outside the "true sampling area" which covers 40% of the actual beam cross section. Optical measurements of the beam diameter in the sampling region and direct measurement of the depth of field which is practically independent of the drop size, lead a good estimate of the true sampling area (0.35 mm^2).

The relation between the particle diameter and the class number is often verified using glass beads, and making corrections due to the refraction index.

b. Direct measurement of the liquid water content (LWC)

The Johnson-Williams (JW) probe manufactured by the Bacharach Instrument Company (sampling area $\sim$16 mm^2) is based on the cooling of a hot wire under constant voltage when impacted by the droplets. The liquid water content is deduced from the variations of the resistance of the wire (Spyers-Duran, 1968).

c. Measurement of the total water content (TWC)

The Ruskin probe manufactured by the General Eastern Corporation (sampling area 75 mm^2) is based on the measurement of the attenuation of Lyman α radiation by the water vapor obtained after evaporation of the droplets and ice crystals on heated grids. The liquid water content can be estimated by

0021-8952/82/020189-08$06.00

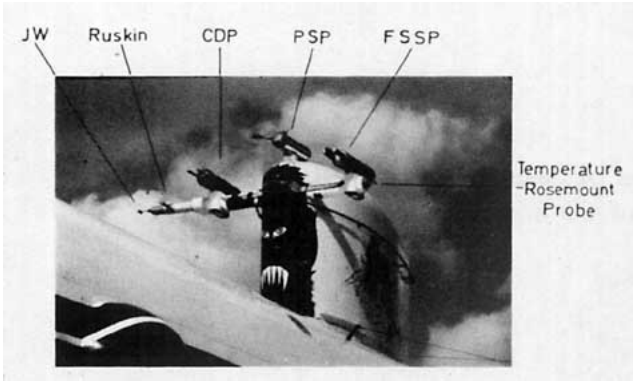

FIG. 1. Location of the different probes on the aircraft: Johnson-Williams (JW), Ruskin, Cloud Droplet Probe (CDP), Precipitation Spectrometer Probe (PSP), Forward Scattering Spectrometer Probe (FSSP), and the Temperature Rosemount Probe.

subtracting the ambient water vapor content, which is deduced from the dew-point temperature.

The mean speed of the aircraft (DC 7) was 100 m s^{-1} and the sampling frequency for these three probes was 10 Hz. Thus the spatial resolution was ~10 m. Fig. 1 shows how the probes are mounted on the aircraft.

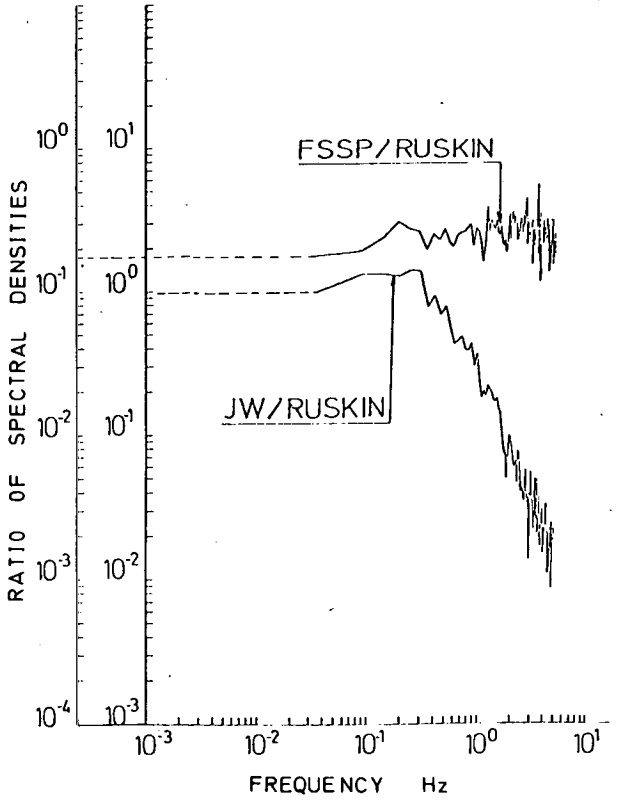

FIG. 2. Ratios of the power spectra of the estimated water content as functions of frequency. Each spectrum is obtained by an ensemble average of six spectra defined on 1024 points (max. freq. 5 Hz) followed by a frequency average, which is computed for 103 frequencies, giving the final spectrum.

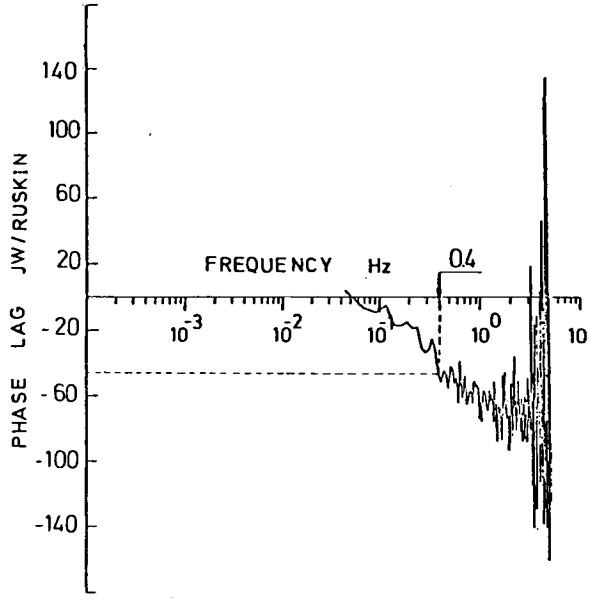

FIG. 3. Phase lag of the power spectra ratio of the JW liquid water content to the Ruskin total water content.

3. Response of the probes

a. Dynamical response of the probes

Fig. 2 shows two ratios of power spectra of water content deduced from the measurements made with different probes during a 20 min flight in a stratocumulus layer. The upper curve corresponds to the FSSP liquid water content compared to the Ruskin total water content and shows that the Ruskin cutoff frequency is at least equal to that of the FSSP (5 Hz). The lower curve corresponds to the JW liquid water content compared to the Ruskin total water content. It shows that the JW probe has a cutoff frequency close to 0.4 Hz, above which the signal is attenuated by 20 dB per decade.[1] This is corroborated by the curve in Fig. 3, in which the phase angle of the cross power spectrum of the JW liquid water content and of the Ruskin total water content is displayed and which shows that a phase lag of 45° is reached at the cutoff frequency. This implies that the JW can be compared to a first-order filter in time which may be due to thermal and electrical inertia.

As a consequence, for the following comparisons, the JW values are averaged over 1 s and the FSSP values recorded every 0.1 s have been smoothed by a recursive first-order filter ($\bar{Y}_n = 0.2Y_n + 0.8\bar{Y}_{n-1}$) and averaged over 1 s. Figs. 4a and 4b give an example of the FSSP liquid water content as a function of the JW liquid water content, during a stratocumulus cloud penetration in a layer near 700 mb

[1] The corresponding characteristic response time of the probe is $t_c = (2\pi F)^{-1} \approx 0.4$ s.

(−10°C), without and with the time smoothing of the FSSP values respectively. They show that the dispersion is reduced by the filtering and justify the subsequent use of smoothed values of the FSSP in the comparison of the liquid water content estimates.

b. Amplitude response of the probes

Figs. 5a and 5b show the Ruskin total water content as a function of the JW and FSSP liquid water contents respectively. Each dot corresponds to a 1 s (~100 m) averaged value during a constant-level flight (700 mb, −10°C) in a stratocumulus cloud (PEP). The points corresponding to a liquid water content >0.05 g m^{-3} are distributed along a line, the slope of which is 0.82 in Fig. 5a and 1.66 in Fig. 5b. The intersection values of these lines with the y axis are close to the water vapor content computed from the dew-point temperature (2.4 g m^{-3}). These figures reveal that, during this penetration, the JW and Ruskin estimations of the liquid water content are in good agreement, whereas the FSSP underestimates this parameter by as much as 40%. During other penetrations, with different microphysical conditions, shown and discussed later, the JW also underestimates the liquid water content.

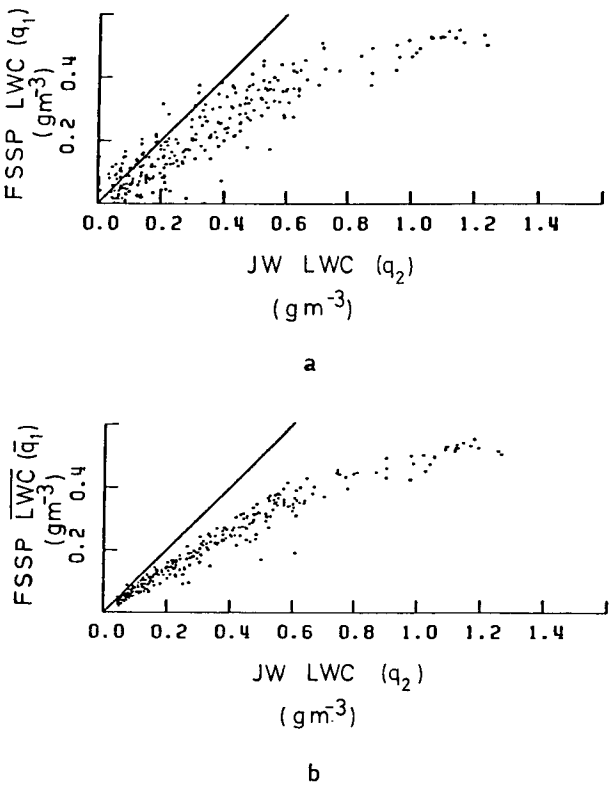

FIG. 4. (a) Unsmoothed and (b) time-filtered FSSP liquid water content as a function of the JW liquid water content. Each dot corresponds to a 1 s averaged value.

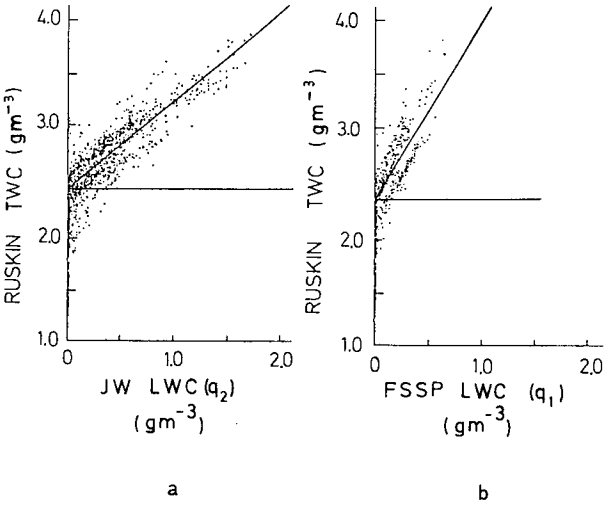

FIG. 5. One-second averaged values of the Ruskin total water content as a function of the corresponding 1 s averaged values of the JW liquid water content (a) and the FSSP liquid water content (b).

4. Analysis of the comparison

With regard to the amplitude response, the discrepancies between the Ruskin and the FSSP result from the electronic circuitry of our FSSP. Any droplet crossing the beam inside an "effective" volume triggers the electronic circuitry which needs a time $\tau = 16$ μs to set itself ready again. During this time, any other particle crossing the beam will not be counted but will again trigger the circuit during 16 μs. This effective volume, which includes the true sampling volume, depends upon the particle diameter and defines the effective beam length L_i corresponding to particles in the ith class. These effective beam lengths L_i may be expected to increase with the diameter since a large particle can give a signal above some threshold further away from the focus plane of the beam. During the time lapse τ, the particle is either counted or rejected if it is outside the true sampling area. It follows that our FSSP undercounts the droplet concentration when the mean time lapse between successive particles approaches 16 μs. Assuming that this time lapse is an exponentially distributed random variable, it can be demonstrated, following Cooper (Breed, 1978), that the measured concentration N_{mj} in the jth class may be expressed as a function of the real concentration N_{0j} by

$$N_{mj} = N_{0j} \exp\left(-\sum_{i=1}^{15} V d \tau L_i N_{0i}\right), \qquad (2)$$

where V is the relative air speed and d the beam width. This relation shows that the total measured concentration N_m ($N_m = \sum_i N_{mi}$) is a function of the total true concentration N_0 ($N_0 = \sum_i N_{0i}$) given by

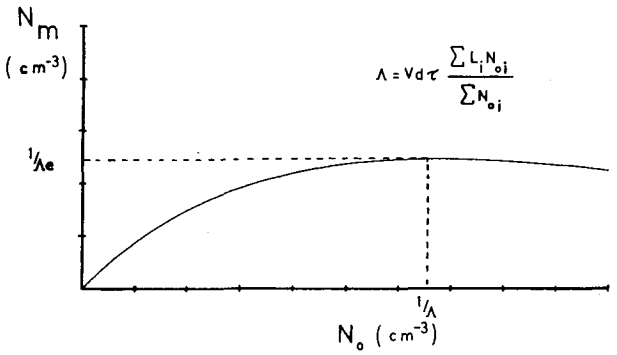

FIG. 6. Measured concentration N_m as a function of the real concentration N_0 [Eq. (2')].

$$N_m = N_0 \exp(-\Lambda N_0), \tag{2'}$$

where

$$\Lambda = \sum_{i=1}^{15} Vd\tau L_i N_{0i} / (\sum_{i=1}^{15} N_{0i}) \quad \text{and} \quad e = 2.718.$$

The value of the parameter Λ depends only on the shape of the droplet size distribution and not on the total true concentration. The previous relation is displayed in Fig. 6 which shows that the total measured concentration cannot exceed the maximum value $(\Lambda e)^{-1}$ which ranges, in our measurements, from 150 cm^{-3} to 350 cm^{-3} depending on the shape of the distribution.

Knowing the droplet size distribution, we can evaluate the true value of the liquid water content q^* as a function of the liquid water content computed from the FSSP q_1 by Eq. (1) as follows:

$$\left.\begin{aligned} q^* \approx q_1^* &= \tfrac{1}{6}\pi \sum_{i=1}^{15} N_{0i} D_i^3 \\ &= (\tfrac{1}{6}\pi \sum_{i=1}^{15} N_{mi} D_i^3)\left(\frac{N_{0i}}{N_{mi}}\right) \\ q_1^* &= q_1 \left(\frac{N_0}{N_m}\right) \\ &= q_1 \exp(\sum_{i=1}^{15} Vd\tau L_i N_{0i}) \end{aligned}\right\}, \tag{3}$$

where the second line results from the fact that the ratio $Y \equiv N_{mi}/N_{0i} = N_m/N_0$ is the same for all classes as shown by Eq. (2).

On the other hand, the JW underestimates the liquid-water content of the large droplets (>30 μm) (Knollenberg, 1972) since the heated wire may not completely evaporate the whole water mass of all impinging water droplets. The large droplets are broken by the wire and the small remainders of droplets are blown away by the aerodynamic effect of the wire. Thus the part of the liquid water measured by the JW decreases with the size of the droplet.

Knowing the droplet size distribution, we can also evaluate the true value of the liquid water content q^* as a function of the liquid water content q_2 measured by the JW by

$$q^* \approx q_2^* = q_2\left(\frac{\sum N_{0i} D_i^3}{\sum N_{0i} D_i^3 \epsilon_i}\right) = q_2\left(\frac{\sum N_{mi} D_i^3}{\sum N_{mi} D_i^3 \epsilon_i}\right), \tag{4}$$

where ϵ_i are the JW underestimation coefficients which depend on the diameters D_i.

In order to obtain realistic values for the coefficient ϵ_i and the effective beam length L_i, we derive a relation between the liquid water content measured by the JW (q_2) and the droplet concentration measured by the FSSP (N_{mi}). This relation is expressed in terms of the parameter Y defined by

$$Y \equiv \frac{N_{mj}}{N_{0j}} = \frac{N_m}{N_0} = \exp(-\sum_{1}^{15} Vd\tau L_i N_{0i}),$$

from which we obtain

$$Y \log Y = -\sum_{1}^{15} Vd\tau L_i N_{mi}, \tag{5}$$

in which Y is computed from

$$Y = \frac{q_1}{q^*} = \frac{q_1}{q_2}\frac{q_2}{q^*} = \frac{\tfrac{1}{6}\pi(\sum N_{mi} D_i^3 \epsilon_i)}{q_2}.$$

These last two relations provide an equation involving the coefficient ϵ_i, the effective beam length L_i, the liquid water content q_2 measured by the JW, and the concentration N_{mj} measured by the FSSP.

A minimization scheme of the sum (~1300 values) of the squared difference between the right and left hand sides of Eq. (5) has been set up as follows, in order to provide an estimate of the unknown parameters ϵ_i and L_i. Due to the nonlinearity of the equation, an "educated" guess estimate of the value of the JW underestimation ϵ_i was provided. The resulting linear system of equations was solved for the 15 values L_i. The initial guess for the ϵ_i was then modified empirically and the set of values which gave the minimum error was retained. A fit of the resulting values of ϵ_i and L_i with smooth analytical expressions was made and the coefficients were further modified in order to provide the minimum error. These values of ϵ_i and L_i are shown in Figs. 7a and 7b.

The decrease of the effective beam length L_i as a function of the droplet diameter was not expected as explained above. However, these coefficients characterize the effective volume of the laser beam which also accounts for the area at the edge of the cross section of the beam in which a particle creates a

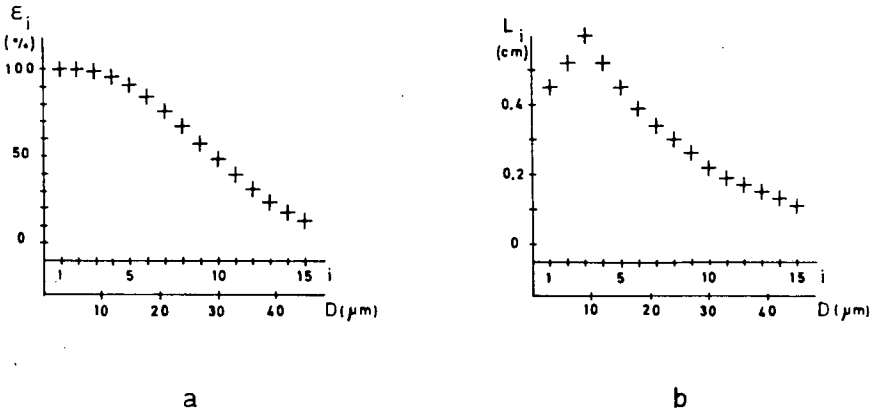

FIG. 7. Values of coefficients ϵ_i (a) and L_i (b) as functions of the droplet diameter D.

signal above some threshold. Further studies indicate that the velocity rejection coefficient (40%) depends on the real concentration and on the droplet diameter. This method of comparison of the measurements lumps together all effects into this one set of coefficients L_i.

From a practical point of view, knowledge of the coefficients ϵ_i does not allow one to compute, with the JW alone, the real value of the liquid water content since the droplet size distribution is not known. However, it is important to know the limitations of the JW as far as the measurements of the liquid water content due to large droplets are concerned.

On the contrary, knowledge of the effective beam length L_i makes possible a good estimation of the real droplet concentration and of the liquid water

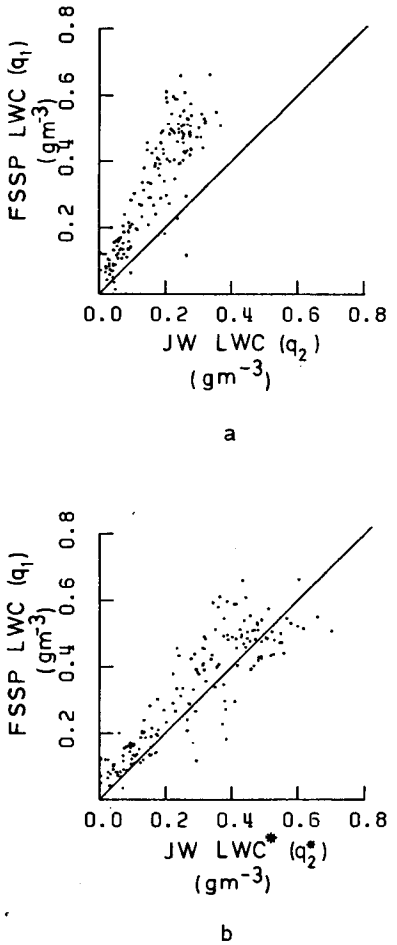

FIG. 8. The FSSP liquid water content as a function of the JW liquid water content (a) without and (b) with correction given by Eq. (4).

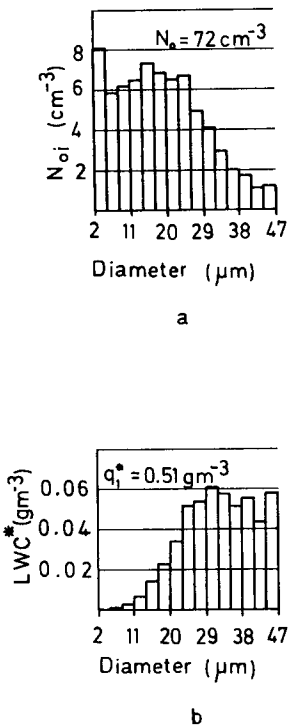

FIG. 9. Size distribution (a) of the droplet concentration and (b) the liquid water content corresponding to one point of Fig. 8.

content with the FSSP alone under the assumption that the true concentration N_0 is lower or equal to the true concentration associated to the maximum measured concentration for given size distribution ($N_m = (\Lambda e)^{-1}$). For our FSSP, the maximum occurs for a true concentration $N_0 = \Lambda^{-1}$ between 400 and 950 cm^{-3}. Furthermore, this correction can be very important since most of our measurement points are situated near the maximum value of N_m, at which the ratio N_0/N_m is equal to e, i.e., ~2.718.

5. Examples of use

a. Underestimation by the JW

An example of the underestimation by the JW is given in Fig. 8a. This figure shows that the JW liquid water is, for this case, lower than the liquid water content computed from the FSSP. The values of the liquid-water content were measured in a cumulus cloud penetration. Ice particles detected by the cloud droplet probe were present in this cloud. But the study of the riming growth, measured by the icing probe, indicates that the droplets are liquid water. During this penetration, the droplet concentration was very low (<100 cm^{-3}) and the underestimation of this concentration by the FSSP is not important.

For one point in Fig. 8a (~100 m in the cloud), we have represented the distribution of the droplet concentration and of the liquid water content as a function of diameter (Figs. 9a and 9b). Fig. 9a shows that the total droplet concentration is not important (72 cm^{-3}); however, the most important part of the

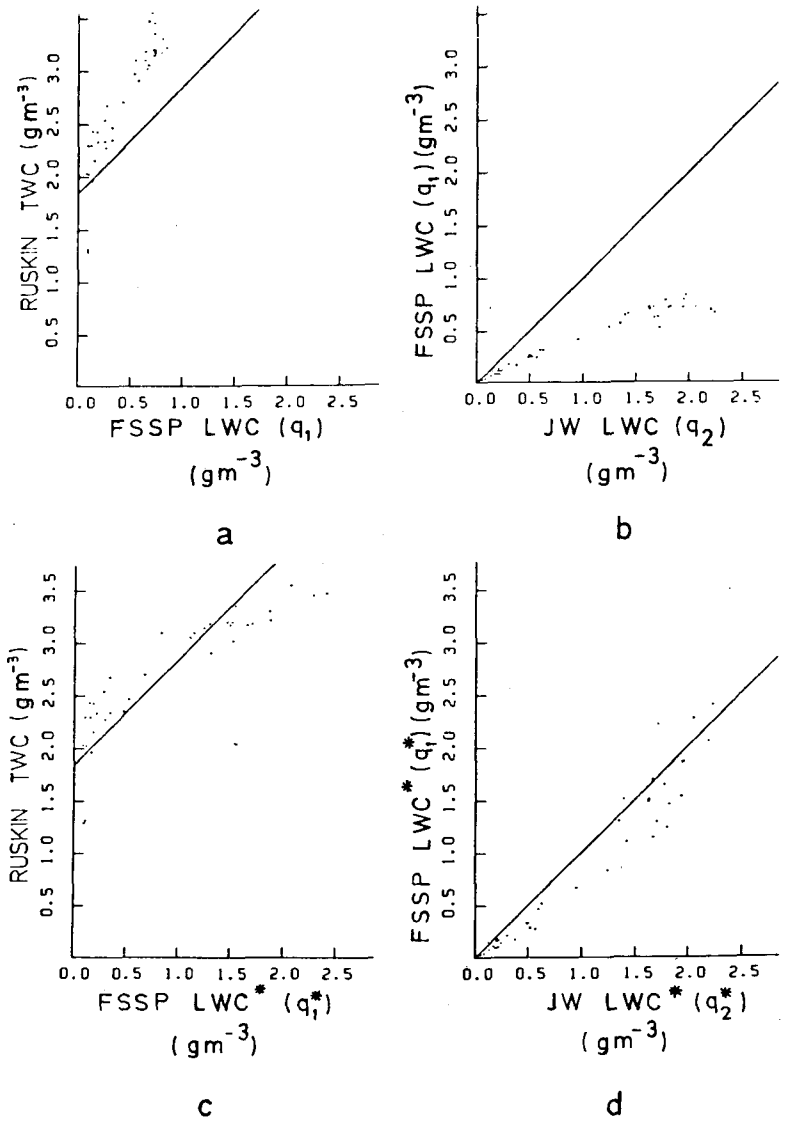

FIG. 10. Comparison of the Ruskin total water content and the FSSP and JW liquid water contents before (*a*, *b*) and after (*c*, *d*) correction (respectively q_1, q_2, q_1^*, q_2^*).

liquid water content ($\sim$0.51 gm^{-3}) is carried by large droplets.

In Fig. 8b, the value of FSSP liquid water content is compared to corrected value of the JW liquid water content [Eq. (4)]. The good agreement between the two liquid water contents clearly implies that the JW probe greatly underestimates the water content due to large droplets and that the relationship given by Eq. (4) can provide a better estimate of the true liquid water content if the droplet distribution is known.

b. Undercounting by the FSSP

An example of undercounting by the FSSP is given in Fig. 10. In Figs. 10a and 10b, the UV total water content (Fig. 10a) and the JW liquid water content (Fig. 10b) are compared to the liquid water content computed from the droplet concentration N_{mj} measured by the FSSP during a constant level flight (700 mb, -10°C) in a cumulus cloud. The droplet concentration was very high ($\sim$700 cm^{-3}) and, as might be expected, the undercounting by the FSSP was significant.

For Figs. 10c and 10d, the values of JW liquid water content are corrected [Eq. (4)] and the FSSP liquid water content is computed with the corrected droplet concentrations N_{0j} [Eq. (2)]. Good agreement can now be seen between the Ruskin, the JW and the FSSP estimates of liquid water content.

c. Results

The last example (Fig. 11) clearly shows the need to use the two correction schemes simultaneously and their success, even under very difficult cloud conditions, in providing good estimates. This example is taken from a penetration at the top of a cumulus cloud at the 620 mb level ($T = -20$°C). This cloud had begun to precipitate and the precipitating particle concentrations measured by the Cloud Droplet and the Precipitating Spectrometer Probes were locally important. It follows that, in addition to the problems dealt with in this paper, i.e., the FSSP undercounting and the JW underestimation, discrepancies between the two types of measurement can result from large particles crossing the FSSP laser beam, and from overestimation by the FSSP of the water content when the particles are frozen water ($\rho < 1$) instead of liquid water ($\rho = 1$). Despite the very low temperature, the discrepancies between the two probes are probably not due to icing: the probes were deiced, the penetration in the cloud was short (2 min) and the value of the mean liquid water content was only 0.4 g m^{-3}. Furthermore, the ice accretion rate measured by the icing probe was 0.3 mm s^{-1} which is below the critical value for the probes (0.7 mm s^{-1}). For this critical value, some problems have been experienced during the PEP experiment.

Fig. 11 displays the time evolution of the mean

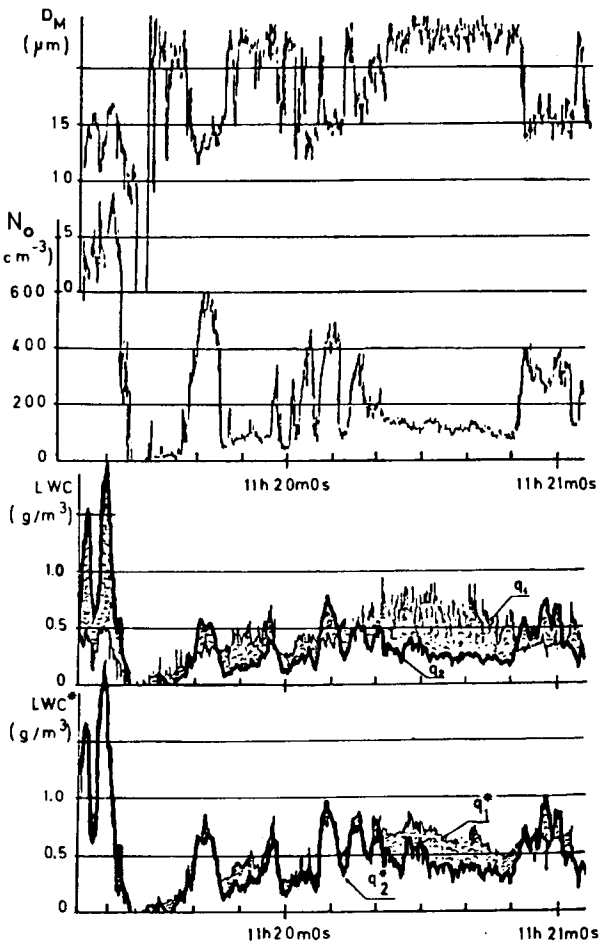

FIG. 11. Time-evolution of the mean volume diameter, the corrected concentration measured by the FSSP, and the FSSP and JW liquid water contents without and with correction. In these last figures the hatched area represents the difference between the two estimates of the liquid water contents.

volume diameter[2] D_M (μm), the corrected droplet concentration N_0 (cm^{-3}), and the liquid water contents (g m^{-3}) computed from the FSSP droplet concentration (q_1) and measured by the JW (q_2), without correction (above) and with corrections (q_1^*, q_2^*) (below). This flight was characterized by a succession of supercooled cells ($N_0 \approx 600$ cm^{-3}, $D_M \approx 15$ μm) embedded in a glaciated and precipitating environment ($N_0 \approx 100$ cm^{-3}, $D_M \approx 20$ μm). These observations are confirmed by other sensors (Ruskin probe, icing probe).

A comparison of the values given by the two probes before correction shows that the FSSP gives a lower value for the liquid water content than the JW in the supercooled cells; the opposite is true in the parts of the cloud containing few large particles. This illustrates clearly the FSSP undercounting and the JW underestimation.

[2] D_M, the mean volume diameter, is computed over the first part of the droplet size spectrum (2 μm $< D <$ 47 μm).

After correction (below) these discrepancies disappeared completely except in the glaciated region where the remaining discrepancies are due to ice particles and a possible overcounting by the FSSP due to large crystals.

6. Conclusions

The Ruskin probe has a cutoff frequency higher than 5 Hz and gives a good estimate of the total water content. However, without a quick-response probe measuring the water vapor content, one cannot deduce the LWC with good accuracy. The JW probe has a frequency cutoff at ~0.4 Hz and the probe underestimates the water content by a factor which depends on the size distribution and which can be computed if this distribution is known. A formula has been suggested which can give a better estimate of the real liquid water content.

Likewise, the FSSP can give a good estimate of the liquid water content of small droplet clouds if the variation of the effective beam length L_i with diameter is taken into account.

Acknowledgments. This research has been carried out under the leadership of Professor Soulage. The authors wish to thank J. F. Gayet, R. Pejoux and D. Rousset for their active collaboration. It was supported by grants from the Délégation Générale à la Recherche Scientifique et Technique and the Direction des Recherches Études et Techniques.

REFERENCES

Breed, D. W., 1978: Case studies on convective storms: 22 June 1976: First echo case. NCAR Tech. Note NCAR/TN-130 + STR, 41-43.

Knollenberg, R. G., 1972: Comparative liquid water content measurements of conventional instruments with an optical array spectrometer. *J. Appl. Meteor.*, **11**, 501-508.

Spyers-Duran, P. A., 1968: Comparative measurements of cloud liquid water using heated wire and cloud replicating devices. *J. Appl. Meteor.*, **3**, 450-460.